IOSR Journal of Mechanical and Civil Engineering (IOSR-JMCE)
e-ISSN: 2278-1684, p-ISSN: 2320-334X, Volume 23, Issue 5 Ser. I (Sep. – Oct. 2026), PP 85-98
www.iosrjournals.org

Aerodynamics of the 2026 FIFA World Cup Match Ball-Trionda: URANS Comparison with Published Wind Tunnel Data and Evolution of World Cup Balls.

Samyak Patni
Sancta Maria International School
Hyderabad, India

Abstract
The Trionda, official match ball of the 2026 FIFA World Cup, is reported to have the lowest critical(drag-crisis) speed for any World Cup ball till date at 11.9 m/s; becoming the most aerodynamically distinctive World Cup ball since the controversial Jabulani in 2010, with the post-crisis drag coefficients of 0.15-0.17. Aerodynamic evidence of Trionda that is published and available is purely experimental; with no consideration of flow-field CFD(Computational Fluid Dynamics) analysis for the ball leaving CFD corroboration unpublished. This paper presents the first CFD characterization of the Trionda through unsteady RANS(Reynolds- Averaged Navier-Stokes) on a photo and data approximated 4 panel geometry, benchmarked against the published wind-tunnel data under pre-allocated convergence thresholds for agreement. This paper uses simulations on a set of 6 speeds from 7 to 30 m/s, from Reynolds Number(Re) $1.0x10^5$ to $4.4x10^5$ to regenerate the qualitative behavior at drag crisis and a post crisis drag. These simulations had identical computational settings. Following this the drag coefficients calculated independently from raw forces were 0.372, 0.329, 0.351, 0.250, 0.289 and 0.219 at 7, 11.9, 15, 20. 25 and 30 m/s respectively. The 41.2% endpoint reduction supports overall regime-dependent drag behavior, although the curve is non-monotonic. Relative to wind-tunnel orientations A and B, the largest positive deviations occurred at 11.9 m/s, the critical speed: +93.6% and +91.3% . At 30 m/s, deviations were −6.6% and +3.1%, satisfying the study's close-agreement criterion for both benchmarks. Agreement was not uniform throughout the high-speed range, however, because deviations at 25 m/s remained +24.9% and +37.4% (in acceptable range). Normalized velocity images showed accelerated flow around the ball and speed-dependent, asymmetric low-velocity wakes, but were used only qualitatively. This discrepancy backtraced to the absence of transition physics in the standard fully-turbulent closures; including the use of URANS and to the estimated surface geometry due to the unavailability of manufacturer CAD. The findings quantize the diagnostic value and the methodological constraints of URANS-only analysis for future World Cup balls.

Keywords: *Trionda; soccer ball/football aerodynamics; drag crisis; critical Reynolds Number; CFD validation; URANS; CAD; 2026 FIFA World Cup.*

I. Introduction

The flight path of a football is influenced by numerous factors not limited to the initial impulse imparted by the kick. These factors include aerodynamic drag, lift and the angular forces; which directly affect the speed, range, dip, curve and stability of the ball in open play and set pieces.

The surface structure of a football, panel topology and surface texture, alter the manner in which the air separates from its surface, playing a vital role in influencing the forces associated with the flight of the ball as it directly affects the wake separation. *The evolution of FIFA World Cup match balls used over the course of the 21st century are clear reflections of the continuous variation in the combination of manufacturing innovation and aerodynamic predictability of the ball.*

1.1 Background of the topic

Since the introduction of the thermally bonded Teamgeist in 2006, each successive tournament ball presented has had fewer panels and modified surface textures: 14-panel Teamgeist in 2006, 8-panel Jabulani in 2010, 6-panel Brazuca 2014, 32-panel Tel-star 18 in 2018, 20-panel Al Rihla in 2022 and most recently the 4-panel Trionda in 2026. Every design faced debates due to the subtle changes in panel count, seam depth, and surface roughness which fundamentally impacted the boundary-layer behavior of air during flight.



The Jabulani (2010) is the most prominent case involving controversy related to the designs of the footballs. The claims of erratic flight path involving sudden lateral movement and the unpredictable 'knuckleball' effect were backed by goalkeepers from various participant countries including Julio Cesar(Brazil), Gianluigi Buffon(Italy), Iker Casillas(Spain),Hugo Lloris(France). Furthermore, multiple outfield players like Robinho(Brazil), David James (England) reported difficulties in controlling shots,long passes and crosses. This ball was defined as 'rotten', 'unpredictable' and 'a beach ball' by the players. On the contrary, the Uruguayan player Diego Forlan had mastered the trajectory of the ball prior to the 2010 world cup and scored several long range goals earning him the player of the tournament and the Golden Boot.

Constructed from merely 8 thermally bonded panels with shallow grooves (total seam length~203 cm and seam depth~0.48 mm), The Jabulani became the smoothest World Cup ball till date as confirmed by the independent free-flight observation by NASA Ames. Aerodynamic investigation post the tournament revealed that the Jabulani's critical Reynolds number was calculated to approximately 18.7 m/s; significantly higher than the ~12.9 m/s critical speed of the traditional 32-panel balls. These findings concluded that the Jabulani underwent an unpredictable zone just as it reached the goalkeeper during the deceleration phase of a nominal 30 m/s shot.



Following this, FIFA and Adidas prioritised surface texture and aerodynamic performance as the key engineering variables during the development of a football over the superficial features, reflected by the deliberate aerodynamic modifications. Subsequently, The Brazuca(2014) rectified the flaws identified in The Jabulani by

increasing the seam depth to ~1.56 mm and the aggregate seam length to ~327 cm, lowering its critical speed to the typical ~12.9 m/s. This design earned positive feedback post the Jabulani. The Trionda(2026) reflects the same engineering ideology: with four-panel construction and enhanced micro-texturing, designed deliberately to be more textured than the recent Al Rihla(2022) and Telstar 18(2018); resulting in the lowest critical speed/drag crisis to 11.9 m/s since the Jabulani.

1.2 Theoretical Background

1.2.1 Aerodynamic Forces

The primary aerodynamic forces are drag, lift, and side force. Drag is the force opposing the motion, lift and side force act perpendicular to the airflow and lead to deviation in the flight path. If a ball spins, the Magnus effect creates pressure difference and causes dip,swerve, or curve.

Drag is given by:

$$F_D = \tfrac{1}{2} \rho V^2 C_D A$$

Where D is ball diameter, ρ is air density, V is air speed, C_D is drag coefficient and A is frontal area.

The Reynolds number is:

$Re = \rho VD/\mu$

Where D is ball diameter and is dynamic viscosity. It helps determine whether the boundary layer around the ball is likely to be laminar or turbulent.

1.2.2 Drag Crisis

During flight air flows over the ball, a thin boundary layer forms near its surface. At lower speeds the flow is smooth and laminar; and at higher speeds it becomes turbulent. This turbulent layer may remain attached farther around the ball which delays flow separation and a decrease in the magnitude of drag. This transition depends on the speed, surface texture, seams, grooves and the orientation.

1.3 Existing Research

Over the past two decades, the development and testing of the World Cup ball has incorporated multiple methods. These methods are used to investigate and analyse specific characteristics and performance data associated with each ball.

Method	How it is used	What it measures
Wind-tunnel Testing	Used to measure actual forces on the physical ball with regulated wind speeds. Used to compare the balls and derive force coefficients for the analysis of the trajectory.	Drag force, lift force, side force, drag coefficient, lift coefficient, critical speed, and aerodynamic behaviour.
Robot-kicking tests	Machines are used to kick the ball under regulated conditions, with the design as the independent variable ensuring an unbiased comparison.	Launch speed, launch angle, spin rate, trajectory, displacement, and accuracy
Player testing	Professional players assess and test the feel of the ball during realistic play.	Touch, grip, passing control, shooting feel, goalkeeper handling and the anticipated ball behaviour
Laboratory durability tests	Ensures the ball can retain its shape and characteristic following continuous impacts and varying weather conditions which helps evaluate if it can have consistent behaviour	Shape retention, pressure retention, seam bonds, bounce, water absorption and resistance to impulse
Computational Fluid Dynamics(CFD)	Aids designing team to assess number of surface textures, seam depths, and panel designs as well as the number of panels before the prototype being produced	Airflow patterns, pressure distribution, boundary layer behaviour, wake formation, flow separation, drag prediction and vortex structures during flight.
Trajectory Simulation	Predicts how the ball will travel post kick with the help of data obtained from wind tunnel.	Predicted flight path, distance covered, flight time, speed loss, and the overall movement derived from the force coefficient data input
High-speed camera analysis	Used by researchers to observe visually how the ball behaves when hit by players or robots.	Ball rotation and spin rate, trajectory, deformation from impact, and movement from field-based kicks
Field testing	Testing the ball in real-world situations with	Real situation performance, predicted and assumed

	multiple factors such as wind, grass, moisture, player techniques and match pressure affecting the overall performance	flight behaviour, player adaptation.

1.3.1 Evolution of World Cup balls over the course of 21st Century

Ball	Panels	~Seam Length(m)	~Seam Depth(mm)	~Critical Speed(m/s)	~C_D	Aerodynamic Affect	Source
Teamgeist(2006)	14	3.45	_	20	0.13	Very Smooth, low-drag design	Asai et al. (2007), Sports Engineering 10(2)
Jabulani(2010)	8	2.01	0.49	21.9-26.9	0.12	Smoothest and least predictable;high critical speed	Hong & Asai (2014), Sports Engineering 17(4); Goff et al. (2011), Physics Today 64(7)
Brazuca(2014)	6	3.30	1.56	14-18	0.17	Deeper seams, textured and better predictability	Hong & Asai (2014)
Telstar-18(2018)	6	4.32	1.10	14-18	0.17	Similar to Brazuca	Hong et al. (2020), Sports Engineering 23
Al Rihla(2022)	20	3.52	1.60	14-18	0.17	Similar to Brazuca and Telstar-18	Hong et al. (2022), Sports Engineering 25
Trionda(2026)	4	_	1.29	11.9	0.17	Lowest critical speed; higher turbulent-regime drag therefore lower long range shot	Hong et al. (2026), Sports Engineering

The Teamgeist was the start of a new chapter in the football development, from traditional 32- panel stitched ball to a brand new 14-panel, that are thermally bonded. This fundamental reconfiguration transformed the ball into a smoother, uniform textured ball that reduced moisture adsorption during the matches. This was followed by the Jabulani that became one of the biggest controversies in the sports equipment development industry and led to deeper research and focus on the design of the ball; mainly the surface texture and aerodynamic behaviour.

The three ball post the Jabulani: Brazuca, Telstar-18 and Al Rihla featured almost similar design and aerodynamic behaviour that was determined to overcome the design flaws of the Jabulani and provide better predictability in flight trajectory. These three had almost identical critical speeds and drag coefficients. Finally, The Trionda has the lowest critical speed and number of panels, high surface roughness and deeper grooves which decreased the ball's shot range but despite this it offered greater performance benefits during open play than the previous designs.

World Cup balls from 2006-2026 were developed and studied using multiple methods including wind-tunnel testing, trajectory simulation or high speed camera analysis, mechanical quality tests and player/robot testing; the manufacturers sole aim remained to create a ball more consistent, durable and predictable in flight than the previous ball. Presently, there are two significant factors influencing recent studies for development of the ball taken from the prior football designs. Firstly, the engineering solution to the flaws identified in the Jabulani to prevent such controversies and ensure it is viable for open play by ensuring the position of the drag crisis relative to the speeds frequently reached in matches. The other factor being, the aerodynamic analysis and evaluation of the balls conducted by employing a combination of various methods such as Wind-tunnel, free-flight tracking, computational fluid dynamics along other scientific techniques due to the complexity and non-monotonic deviation in airflow associated with the ball.

1.3.2 The Trionda(2026)

Goff et al. tested Trionda in a wind tunnel and reported a critical speed of 11.9 m/s in two orientations[1]. They recorded drag coefficients ranging from 0.15 to 0.17 at the measured critical speeds, not inclusive of the

post-critical range. These experimentally measured coefficients were used in their trajectory model instead of the values obtained from solving the flow field using CFD. Following that Hong et al. demonstrated that the drag behavior of the Trionda can vary significantly with the orientation considered during the study[2]. The results from these two researches set an experimental benchmark along with the clarification that a computational comparison must not treat the ball as orientation-independent.

Use of Flow-field CFD provides the estimated integrated forces while also generating velocity, pressure and wake information that is challenging to obtain from a global force measurement independently. Even after this CFD predictions depend on geometry fidelity, orientation considered, the mesh used and temporal resolution of the simulation, turbulence treatment and method of force-averaging. Hence a cross-method study can quantify where agreement occurs and where it is not supported instead of speculating that a visually coherent wake validates the computed drag.

1.4 Research Gap

The Trionda is the first World Cup ball for which the officially published aerodynamic analysis is purely experimental with no officially published research using CFD flow-field simulations performed on Trionda's newly implemented geometry and surface texture. The current study only utilises the trajectory tracking simulations run using the coefficient values obtained from wind-tunnel experiment. Therefore the gap this paper addresses is the methodological corroboration: to what extent can independently reconstructed Trionda CFD model, simulate independently on the estimated geometrical design with standard turbulence modeling, substantiate the published orientation dependent wind-tunnel aerodynamic behavior of the Trionda? The study does not rely on an unverified claim that no other CFD work exists.

1.4 Research Questions

Primary Research Question **-** How well does a non-spinning URANS model of a reconstructed Trionda geometry corroborate published wind-tunnel drag coefficients over 7-30 m/s when all the computational settings except the velocity in-let are held constant?

Secondary Research Question - How do the computed drag pattern and qualitative wake structure of the simulations vary over the considered speed range, and what do these deviations imply about the credibility of the model for transition-region and high-speed assessment?

1.5 Hypotheses and Agreement Criteria

These hypotheses were refined based on preliminary simulations and are assessed transparently against the final 6 speed dataset.

H1 - Overall drag reduction **-** CFD will produce a substantially lower drag coefficient at 30 m/s compared to that at 7 m/s and one or more significant drag reduction in interim values, consistent qualitatively with the regime-dependent drag behaviour. Monotonic/Unidirection decrease is not required.

H2 - Transient region discrepancy - The most positive CFD-Wind tunnel variation will be approximately near the experimentally reported critical speed of 11.9 m/s.

H3 - Highest-speed agreement - The cross-method analysis will be in agreement at 30 m/s, corresponding to Re= 4.4×10^5. With the computed drag coefficient being similar to drag coefficients in both wind-tunnel orientations within the 20% limit of practical accuracy.

Signed Deviation = 100(Cd[CFD] – Cd[WT])/(Cd[WT])

Note: Absolute deviation of ≤10% suggest close agreement
Absolute deviation of ≥10% and ≤20% suggest partial agreement
Absolute deviation of ≥20% suggest discrepancy
These are considered and refined post preliminary simulations.

II. Methodology

2.1 Study Design

A single reconstructed Trionda geometry and orientation were simulated without spin at 7, 11.9, 15, 20, 25, 30 m/s. Identical computational settings were used for all the six runs, with only the In-let Velocity or Freestream Speed as the set run variable. The study consists of a combination of computational drag prediction, independent

coefficient post-processing, external experimental benchmarking and qualitative velocity field comparison. No original wind tunnel or drop test measurements have been conducted.

2.2 Geometry, Reference values and Post processing

The Trionda ball geometry was reconstructed from public imagery and published numerical data due to the unavailability of manufacturer CAD. The Trionda is a four panel construction[3]. Seam and surface-texture details remain approximate. The reference diameter was D = 0.220 m, giving projected area $A = \pi(D/2)^2 = 0.038013$ m². Air density and kinematic viscosity were $\rho = 1.225$ kg/m³ and $\nu = 1.5 \times 10^{-5}$ m²/s. Reynolds number was calculated as $Re = VD/\nu$.

Drag coefficients were calculated manually using $Cd = 2F/(\rho V^2 A)$, where F is the reported drag force. Dynamic pressure was calculated as $q = 0.5\rho U^2$. This independent calculation verifies coefficient arithmetic and ensures a common post-processing convention across speeds. It does not, by itself, establish grid independence or physical validation.

2.3 Experimental Benchmark and Digitization

Experimental values were digitized from the Trionda curves in Figures 6 and 7 of Goff et al. [1]. Figure axes were calibrated using the published speed and drag scales, and the centers of the Trionda markers were read at the six CFD speeds. The 11.9 m/s comparison uses the experimentally identified critical-speed minimum. Values are therefore approximate digitized measurements rather than authors' raw data.

The CFD orientation could not be matched uniquely to either experimental orientation. Results are consequently reported against orientation A and orientation B separately, forming a comparison group rather than a single averaged benchmark. Comparisons were made at exact nominal speeds. Goff et al. used $\nu = 1.55 \times 10^{-5}$ m²/s, whereas the CFD post-processing used 1.5×10^{-5} m²/s; the resulting Reynolds-number convention difference is acknowledged as a limitation [1]. Experimental error bars were not propagated into the deviation calculations.

2.4 Velocity Field processing

Solution field images were supplied for 7, 11.9,15, 20, 25 and 30 m/s. To avoid misleading comparisons caused by different automatic color limits and image magnifications, each field was remapped to normalized velocity magnitude $|V|/U\infty$ and aligned using ball diameter as the common length scale for 5 speed excluding 15 m/s. The panels utilise a common colour range to ease the ability to compare. The resulting panels use a common color range. Because the source images are snapshots rather than demonstrated time averages, the analysis is restricted to qualitative wake morphology rather than nominal value consideration. Wake length, separation angle/direction and vortex shedding rates are not measured and not considered to make assessments.

2.5 Bias and Effectiveness

The constancy in the settings and designs enables an unbiased and fair intercomparison of the sample speeds. This paper is presented as entirely a comparative pilot study rather than an uncertainty backed predictive model. This constraint is carried through Results, Discussion and Conclusion.

III. Results

3.1 Computational Drag Coefficients

Table 1 depicts the six computational runs with corresponding data and variable values.

Table 1. CFD forces, dynamic pressure, Reynolds numbers and independently calculated drag coefficients.

V (m/s)	Re (x10^5)	F (N)	q (Pa)	Cd
7	1.027	0.4240	30.01	0.371645
11.9	1.745	1.0859	86.74	0.329044
15	2.200	1.8400	137.81	0.351232
20	2.933	2.327	245.00	0.249859
25	3.667	4.2000	382.81	0.288621
30	4.400	4.5800	551.25	0.218566

There is a decrease in the Cd of 41.2% through the sample from 7 m/s to 30 m/s, but the deviation is non-monotonic.

Table 2. Percentage changes between the sample speeds

ΔV (m/s)	Percentage change(%)
7 - 11.9	– 11.5
11.9 - 15	6.7
15 - 20	– 28.9
20 - 25	15.5
25 - 30	– 24.3

The local maximum occurs at 15 and 25 m/s from the sampled set. Due to these fluctuations/ oscillations the resulting curve can not be termed as a single monotonic drag crisis transition.

3.2 Comparative Analysis between CFD & Wind Tunnel data

Table 3. Speed matched comparison with the digital approximates of wind tunnel values from Goff et al.[1]

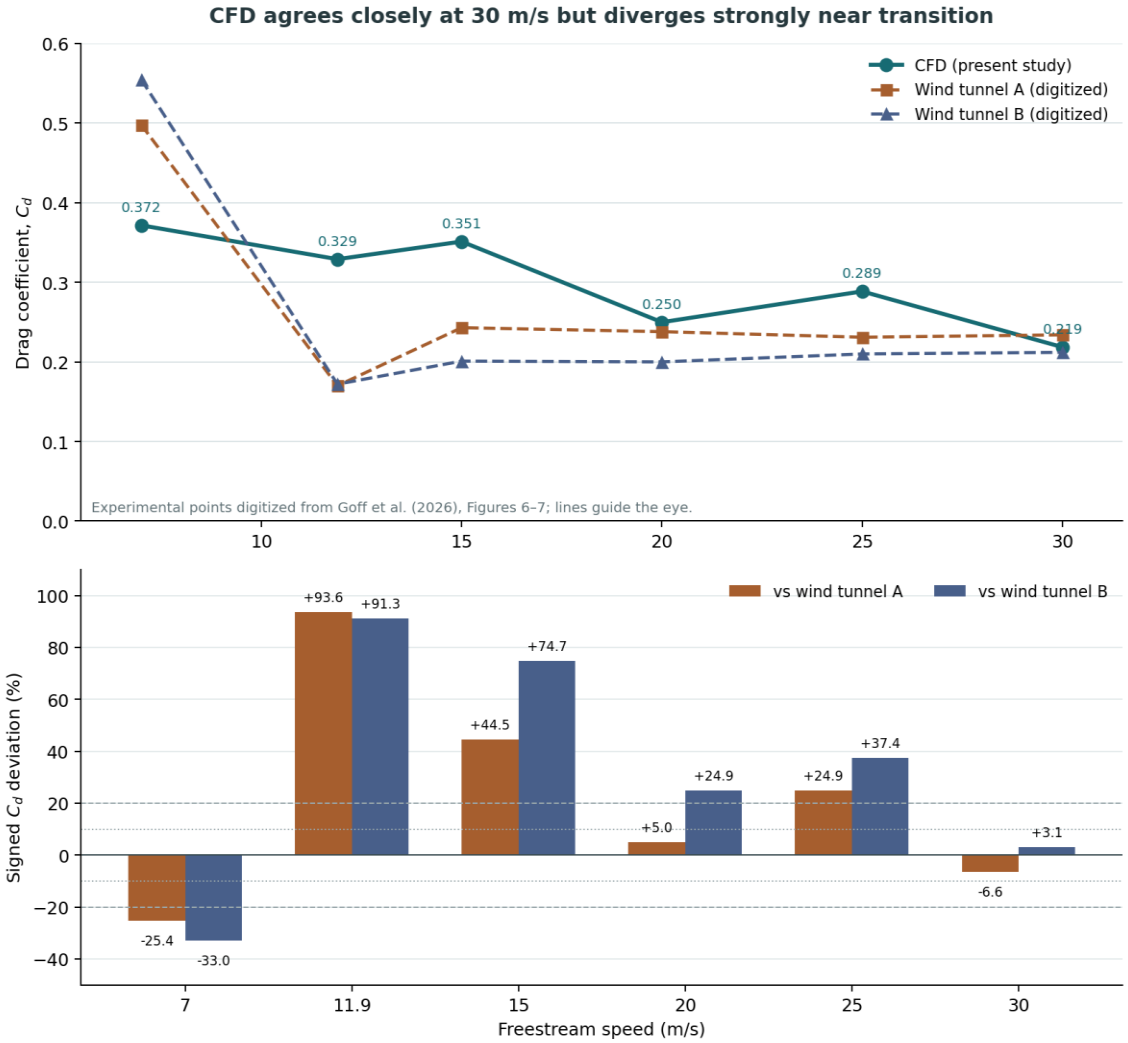
V (m/s)	WT A	Dev. A (%)	WT B	Dev. B (%)	Analysis
7	0.498	– 25.4	0.555	– 33.0	Discrepancy A & B
11.9	0.170	93.6	0.172	91.3	Discrepancy A & B
15	0.243	44.5	0.201	74.7	Discrepancy A & B
20	0.238	5.0	0.200	24.9	Close A only
25	0.231	24.9	0.210	37.4	Discrepancy A & B
30	0.234	– 6.6	0.212	3.1	Close A & B

WT A= Wind Tunnel Orientation A, WT B= Wind Tunnel Orientation B,
Dev.= Signed CFD deviation relative to the stated experimental orientation
The digitized values are approximates and not nominal.

Table 4. Analysis of Dev.

V (m/s)	Dev. Description
7	Underpredicts
11.9	Overpredicts significantly(largest)
15	Overpredicts significantly
20	Very close to A, Similar to B
25	Overpredicts
30	Best predictions: under for A, over for B

The comparison therefore does not support a uniform positive offset or a general statement that accuracy improves monotonically with speed. Instead, it identifies localized agreement at 20 m/s for orientation A and at 30 m/s for both orientations, alongside substantial low-speed and transition-region disagreement.



3.3 Hypothesis Assessment

Table 5. Final Assessment of the Hypotheses

Hypothesis	Result	Evidence
H1 - Overall drag reduction	Supported	Cd is 41.2% lower at 30 m/s than 7 m/s; there are significant decreases over 15-20 and 25-30 m/s. Curve not monotonic.
H2 - Transient region discrepancy	Supported	Deviation at 11.9 m/s are +93.3%(A) & +91.3%(B); Largest positive values in sample
H3 - Highest-speed agreement	Supported	Deviation at 30 m/s are –6.6%(A) & +3.1%(B); both in close agreement.

The Results are only directed to the stated Hypotheses and points. H3 does not infer agreement throughout the post critical regime and H1 is not a demonstration that computed critical matches 11.9.

3.3 Solution Fields for Qualitative Velocity-Field behaviour

Here are the individual solution fields of each sample speed with a scale for velocity magnitude at the bottom of the figure.

Figure 2. 7 m/s Solution Field

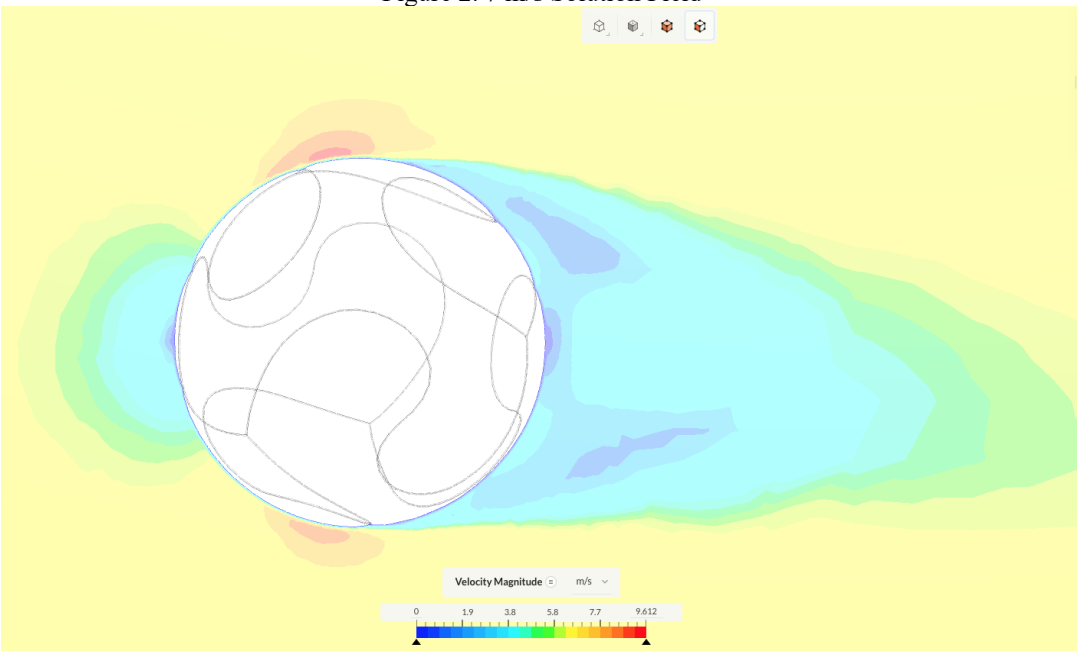


Figure 3. 11.9 m/s Solution Field

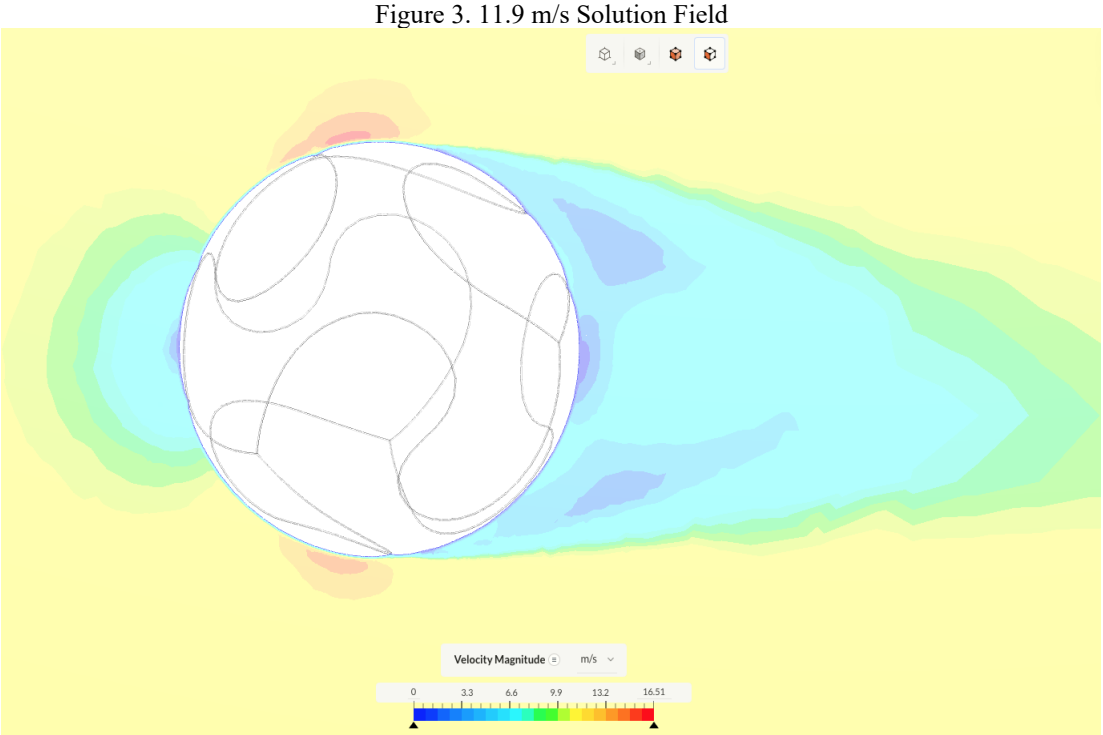


Figure 4. 15 m/s Solution Field

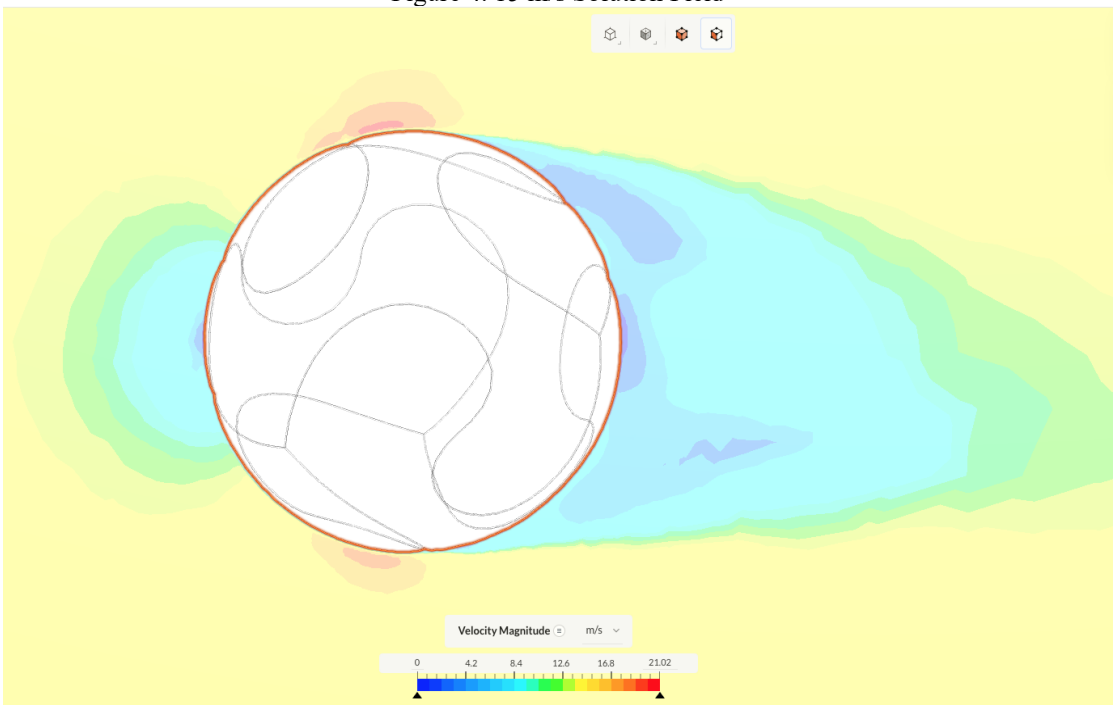


Figure 5. 20 m/s Solution Field

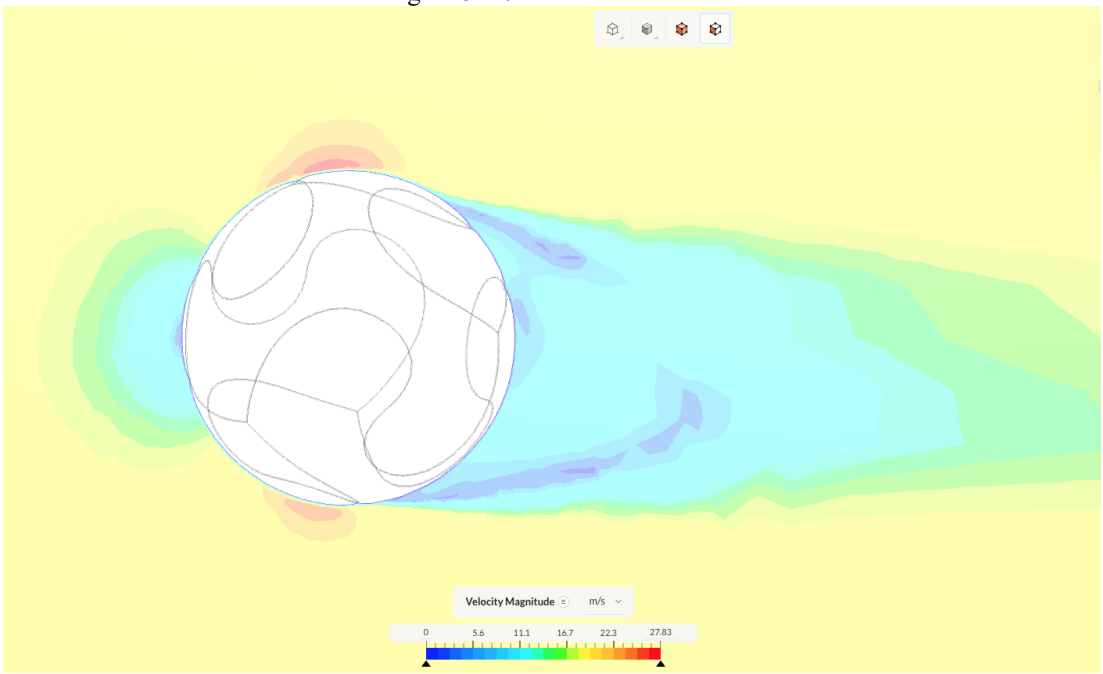


Figure 6. 25 m/s Solution Field

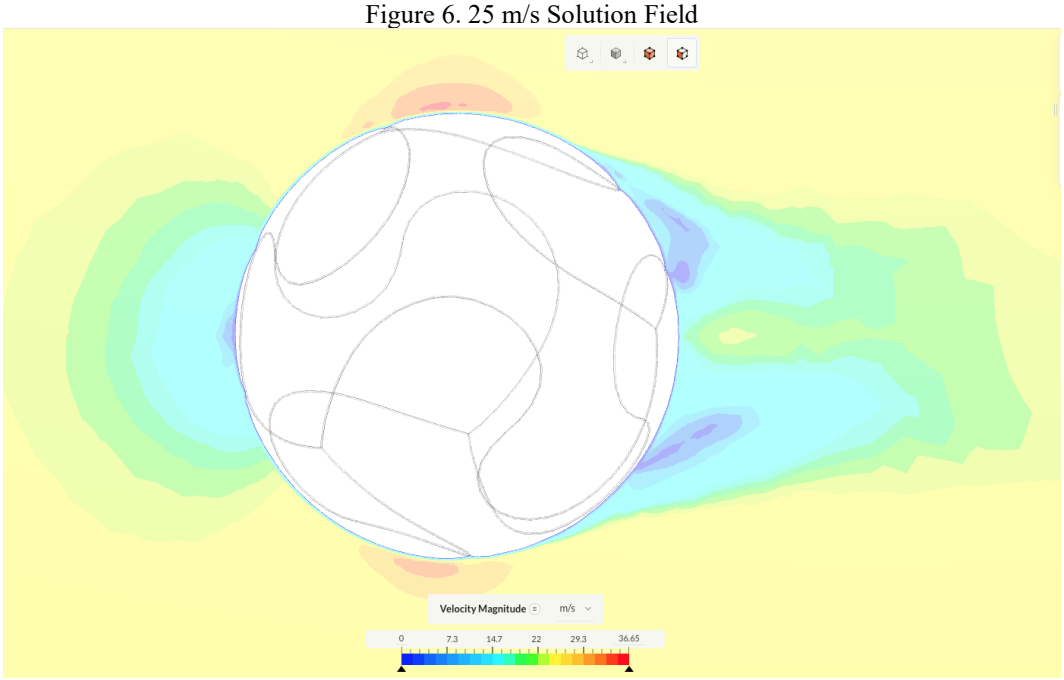
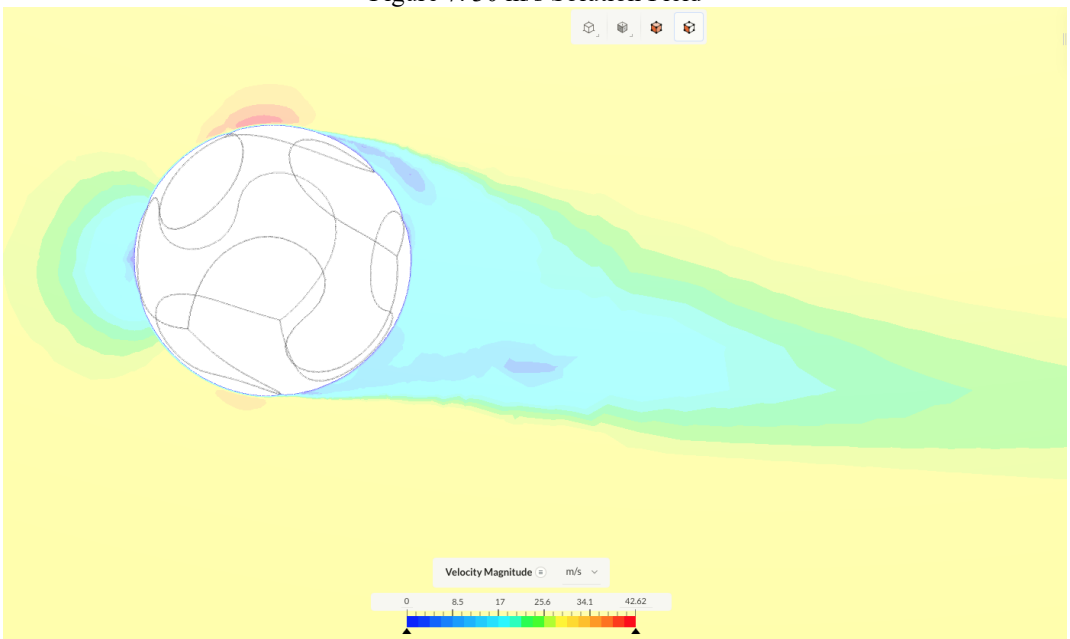


Figure 7. 30 m/s Solution Field



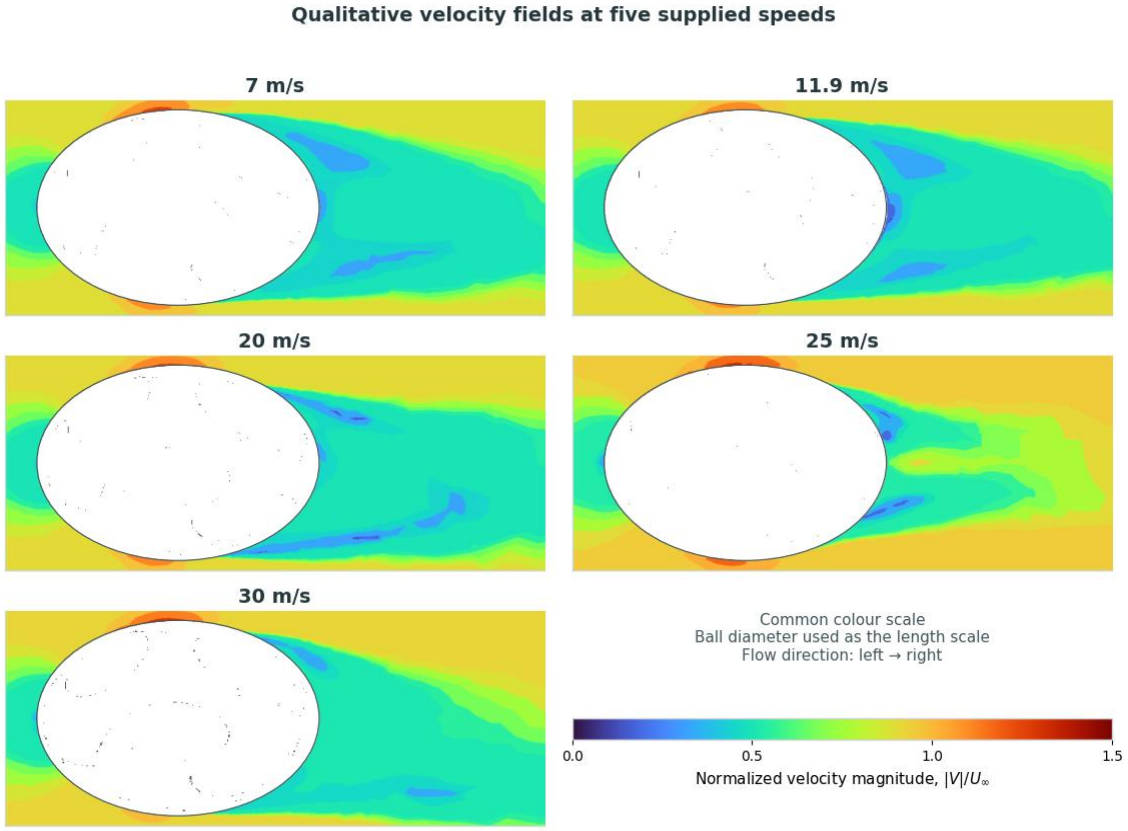


Figure 8. Normalized velocity magnitude fields at five of the sample speed,
excluding 15 m/s,
Color represent |V|/U∞ on a common scale: panels are aligned by the ball diameter

The five solution fields show accelerated flow around the upper and lower shoulders of the ball and a low velocity region downstream. The wake is asymmetric and contains distinct low speed pockets whose position and shape differentiates with speed. The 7 and 11.9 m/s fields are almost identical in normalized form. At 20 m/s, a significantly longer lower wake low speed region is visible. The 25 m/s field appears more fragmented and shortened, whereas the 30 m/s field shows a more continuous and longer downstream low speed region.

These observations demonstrate speed dependent wake morphology, but they do not establish a monotonic change in wake size or an explanation for the drag coefficients which can be influenced by multiple factors. No quantitative separation or wake-length is measured or any claim is made.

IV. Discussion

4.1 Interpretation of drag curve

The focal computational data is an overall reduction in drag along with noticeable reversal in the trend over intermediate values. The complex bluff body response to the variation in Reynolds number can explain the behaviour, nevertheless merely six samples provide insufficient data to come to a reliable critical speed. Therefore the conclusion that can be made is based on the regime dependent drag behaviour rather than validating the drag crisis curve using exact values.

The drag forces show a consistent rise over the sample speeds from 0.424 N at 7 m/s to almost 10x, 4.58 N at 30 m/s. The fall in Cd is the aftermath of lower rate of increase of drag force relative to the dynamic pressure; not due to the fall in absolute drag force. This proves to be an essential factor in determining the coefficient trend accurately.

4.2 Speed & Orientation Dependent Agreement

The comparative analysis can be classified into three category:
1)CFD underpredicting Cd at 7 m/s relative to both orientations.

2)CFD overpredicting Cd significantly near the transient phase, with the maximum positive discrepancy at 11.9 m/s.
3)The high speed agreement which is mitigated to specific regions where at 30 m/s the Cd is in close agreement with both the orientations.

Orientations changes the interpretation at 20 m/s; same CFD result that is in close agreement(~5%) of orientation A is however in discrepancy(~25%) with orientation B, suggesting that averaging the two experimental curves or comparison against an average Trionda drag value can ignore a considerable source of uncertainty.

4.3 Possible Cases of Anomaly

The results overlook a rare constancy factor. The transition sensitive turbulence modeling is a plausible factor close to the critical regime due to the standard RANS closures not representing laminar to turbulent transition accurately and in the correct manner. A correlation based transition model is one case of future modeling approach[4]. However, the comparison present can not separate that effect from the reconstructed seam depth, approximated texture, orientation disparity, time step choice or experimental uncertainty.

Furthermore, the data validate the statement that the current model is unable to reproduce the transient region drag. They do not support the more significant statement that a particular turbulence model has been proven responsible. To add to that, the close agreement at 30 m/s is still insufficient to verify every part of the flow field.

4.4 Implications for CFD based Ball Assessment

The method's value is in comparative and diagnostic analysis rather than an absolute certification, by illustrating the drag and wake morphology change in a controlled system and generating computationally acquired comparisons against the experimental data. Contrariwise, the extensive transient region deviation showcases the limitation because of which similar models should not be used without credibility and proper analysis to derive a critical speed. The wind tunnel method still remains essential for reliable experimental classification, while the CFD can be a method to corroborate the findings by providing in depth flow field details to enhance the results.

V. Methodological Contribution

This study contributes a transparent and unbiased cross method procedure: raw force coefficient reconstruction using identical settings in speed comparison against two experimental orientations individually with hypothesis assessment and normalized qualitative flow illustration. Following this procedure provides two differing ways to assess: arithmetic checking and visual or physical analysis.
Secondly, it demonstrates that agreement can be heavily influenced by speed and orientation given the variation between 11.9, 25 and 30 m/s suggesting that match ball CFD should be simulated over a range of velocity.

VI. Limitations and Future Improvements

Geometry and Orientation: Unavailability of manufacturer CAD resulted in the use of seam and texture geometry that were estimates. Moreover the simulations were done on only one computational orientation and the CFD orientation could not be aligned exactly with the experimental orientations A and B.

Speed Resolution: Six speeds do not provide enough data to come to a valid conclusion especially when resolving for the critical region.

Experimental Comparison: Wind Tunnel results had to be digitised approximately from the accurate published figures. Experimental scatters and error bars were not propagated, while there was also use of equal magnitude speeds despite small variation in the air property conventions.

Flow Field evidence: Image normalization enables qualitative comparison but does not convert screenshots into time averaged quantitative wake measurements(purely visual).

Physical Scope: The model is non spinning and does not predict normal forces, Magnus effects or Trajectories.

For future improvements the priorities should be considering mesh verification, orientation based geometry, denser transient region sampling and controlled turbulence/transition model evaluation. Other essential focus factors include and are not restricted to: surface texture scans, additional orientations, spinning factor and trajectory modeling that will only be beneficial post the major limitations listed have been rectified or mitigated significantly.

VII. Conclusion

URANS simulations of a reconstructed, non spinning Trionda over six identical settings produced Cd of 0.372, 0.329, 0.351, 0.250, 0.289 and 0.219 at 7, 11.9, 15, 20. 25 and 30 m/s respectively. The endpoint coefficients have a 41.2% reduction in Cd which corroborates overall regime dependent drag behaviour; however, the non conforming intermediate values prevent a simple unidirectional crisis interpretation.

Comparison with two published wind-tunnel orientations showed strong speed dependence. CFD under-predicted drag at 7 m/s, over-predicted it most strongly at 11.9 m/s by 93.6% and 91.3%, and remained discrepant at 25 m/s. At 30 m/s, however, deviations were only −6.6% and +3.1%, meeting the close-agreement criterion for both orientations. The operational hypotheses concerning overall drag reduction, maximum positive discrepancy near 11.9 m/s and agreement within 20% at 30 m/s were supported.

The study's defensible conclusion is therefore limited but useful: the present model can reproduce high-speed integrated drag closely at a tested operating point, yet it does not reproduce transition-region behavior or establish a reliable critical speed. URANS should be treated as a complement to wind-tunnel characterization, with geometry, orientation and numerical uncertainty explicitly controlled before broader predictive claims are made.

References

[1]. Goff, J. E.; Hong, S.; Liu, R.; Asai, T. Trionda: Enhanced Surface Roughness Relative to Previous FIFA World Cup Match Balls. Applied Sciences 2026, 16, 2808. https://doi.org/10.3390/app16062808.
[2]. Hong, S.; et al. Orientation-Dependent Drag Crisis and Post-Critical Aerodynamics of the 2026 FIFA World Cup Ball (Trionda). Applied Sciences 2026, 16, 4384. https://doi.org/10.3390/app16104384.
[3]. FIFA. FIFA Celebrates Launch of Official Match Ball of FIFA World Cup 26: TRIONDA. 2 October 2025.
[4]. Menter, F. R.; Langtry, R. B.; Likki, S. R.; Suzen, Y. B.; Huang, P. G.; Völker, S. A Correlation-Based Transition Model Using Local Variables—Part I: Model Formulation. Journal of Turbomachinery 2006, 128, 413–422. https://doi.org/10.1115/1.2184352.
[5]. Data availability: All CFD values and digitized experimental values used in the analysis are reported in Tables 1 and 3. The experimental curves remain subject to the accuracy of figure digitization and the original publications [1,2].